

SYNTHESIS, SINGLE CRYSTAL STRUCTURE, AND HIRSHFELD SURFACE OF (*E*)-*N*'-(2-HYDROXYBENZYLIDENE)-2-((3-(TRIFLUOROMETHYL)PHENYL)AMINO)BENZOHYDRAZIDE

Hanifi Özşanlı^{1*}, Sude Saral Çakmak², Ufuk Çoruh¹, Sevgi Karakuş³, Ezequiel M. Vazquez-Lopez⁴

¹Ondokuz Mayıs University, Faculty of Sciences, Department of Physics, 55200, Atakum, Samsun, Turkey

²Department of Pharmaceutical Chemistry, Faculty of Pharmacy, Marmara University, 34854, Istanbul, Turkey

³Department of Pharmaceutical Chemistry, Faculty of Pharmacy, Istanbul Aydın University, 34295, Istanbul, Turkey

⁴Universidad de Vigo, Departamento de Química Inorganica, Facultade de Química, 36310, Vigo, Spain

2021hanifiozsanli@gmail.com

A hydrazide-hydrazone derivative, (*E*)-*N*'-(2-hydroxybenzylidene)-2-((3-(trifluoromethyl)phenyl)amino)benzohydrazide, was synthesized and characterized using various spectroscopic techniques such as FTIR, ¹H-NMR and ¹³C-NMR spectroscopy, and X-ray diffraction. The compound crystallized in the monoclinic space group *P*2/*n*, with lattice parameters: *a* = 21.0586(8) Å, *b* = 8.1969(3) Å, *c* = 21.6475(10) Å, and β = 92.886(2)°.

Within a single crystal cell, two crystallographically independent asymmetric molecules are present. These molecules are chemically identical but display a non-planar geometric molecular structure. The crystal structure was stabilized by C–H···O and C–H···N hydrogen bonds, which facilitate intermolecular interactions that form a three-dimensional network. The presence of effective hydrogen bond donors and acceptors contribute to the formation of a tightly interconnected three-dimensional structure. Additionally, Hirshfeld surface analysis was conducted to examine potential hydrogen bonding and spatial arrangement of atoms. This analysis quantified hydrogen bond interaction and identified atoms likely to participate in such interactions. Alongside stabilization by strong hydrogen bonds, π ··· π interactions significantly influence the packing arrangement, with interactions among the phenyl rings observable through shape index and curvedness diagrams.

Keywords: crystal structure; X-ray diffraction; Hirshfeld surface analysis; fingerprint plots; hydrazide-hydrazone

СИНТЕЗА, КРИСТАЛНА СТРУКТУРА И АНАЛИЗА НА ХИРШФЕЛДОВА ПОВРШИНА НА (*E*)-*N*'-(2-ХИДРОКСИБЕНЗИЛИДЕН)-2-((3-(ТРИФЛУОРОМЕТИЛ)ФЕНИЛ)АМИНО)БЕНЗОХИДРАЗИД

Синтезиран е дериват на хидразид-хидразон, (*E*)-*N*'-(2-хидроксибензилиден)-2-((3-(трифлуорометил)фенил)амино)бензохидразид и направена е негова карактеризација со користење на различни спектроскопски техники: FTIR, ¹H-NMR и ¹³C-NMR спектроскопија и рендгенска дифракција. Соединението кристализира во моноклиничната просторна група *P*2/*n*, со параметри на ќелијата: *a* = 21,0586(8) Å, *b* = 8,1969(3) Å, *c* = 21,6475(10) Å и β = 92,886(2)°. Во една кристална ќелија, се присутни две кристалографски независни асиметрични молекули. Овие молекули се хемиски идентични, но покажуваат непланарна геометриска молекулска структура. Кристалната

структура е стабилизирана со водородни врски C–H...O и C–H...N кои ги олеснуваат интермолекуларните интеракции, образувајќи тридимензионална мрежа. Присуството на ефективни донори и акцептори на водородни врски придонесува за формирање на стегнато поврзана тридимензионална структура. Дополнително, беше спроведена анализа на Хиршфелдова површина, за да се испита потенцијалното поврзување преку водородна врска и просторниот распоред на атомите. Оваа анализа ја квантифицираше интеракцијата на водородните врски и идентификуваше атоми кои веројатно учествуваат во таквите интеракции. Покрај стабилизацијата со силни водородни врски, $\pi\cdots\pi$ интеракциите значително влијаат на распоредот на пакувањето, при што интеракциите меѓу фенилните прстени можат да се регистрираат преку дијаграмите на индексот на обликот и на заобленоста.

Клучни зборови: кристална структура; рендгенска дифракција; анализа на Хиршфелдова површина; графици на отпечатоци на прсти; хидразин-хидразон

1. INTRODUCTION

Schiff bases represent compounds distinguished by the presence of carbon-nitrogen double bonds, which arise from the nucleophilic addition reaction between amines and aldehydes or ketones.¹ The bond formed when an amine reacts with an aldehyde is called an azomethine bond, while the bond resulting from reaction with a ketone is referred to as an imine bond.² Also known as imines, Schiff bases have become noteworthy due to their stability and ease of synthesis, making them compounds of interest.^{2–4}

Hydrazones contain a specific functional group characterized by the C=N double bond and an NH₂ group, which is part of the hydrazone functional group. They are interesting functional groups of significant importance in chemistry, displaying remarkable biological activity in organic chemistry due to the presence of the azomethine group (N=CH).^{5,6} The activity of these compounds is attributed to the presence of the azomethine group and other surrounding subunit groups.⁷ They are produced by the reaction of aldehydes and ketones with the –NNH₂ group⁸ and are defined by the presence of an (HN–N=C) linkage between two aromatic phenyl rings.⁹

Hydrazones are an important category of ligands with binding properties attributed to various coordination sites, typically coordinated through oxygen and nitrogen atoms to create an environment similar to biological systems.^{10,11} The fact that some of the newly synthesized hydrazones have biological activity,¹² such as antimicrobial,¹³ anticonvulsant,¹⁴ analgesic,¹⁵ anti-inflammatory,¹⁶ antiplatelet,¹⁵ antituberculosis,¹⁷ and anticancer¹⁸ effects, has attracted significant research interest in this field.

The hydrazone group, with its structural and functional diversity, exhibits: (i) nucleophilic imine and amino-type nitrogens, which are highly reactive; (ii) an imine carbon with both electro-

philic and nucleophilic properties; (iii) configurational isomerism due to the unique nature of the C=N double bond; and (iv) N–H-type acid and proton-donating properties.¹⁹ These structural motifs define the physical and chemical properties of the hydrazone group and are crucial in determining its range of applications.

Similar in structure to imines, hydrazones exhibit greater stability, primarily attributed to mesomeric effects that reduce the electrophilicity of the C=N bond. Under normal conditions, hydrazones are considered kinetically inert, even in pure water, with optimal stability in the pH range of approximately 5–11. However, they are susceptible to all three types of reactions observed in imines: (i) exchange; (ii) metathesis; and (iii) hydrolysis.²⁰

In addition to assessing individual molecular characteristics, it is crucial to investigate intramolecular effects. This exploration aids in comprehending how interaction points influence the geometric attributes of individual molecules. Furthermore, Hirshfeld surface analysis provides valuable insights into determining whether a crystal demonstrates polymorphic properties.²¹

The compound discussed in this article was systematically produced in the same manner as part of the synthetic discovery of numerous other organic analogs in a French patent.²² In this patent, the title compound is labeled as compound number 30. The purpose of this article is to re-synthesize the compound, (*E*)-*N'*-(2-hydroxybenzylidene)-2-((3-(trifluoromethyl)phenyl)amino)benzohydrazide, to elucidate its molecular geometry by performing single crystal X-ray diffraction (XRD) analysis. This hydrazide-hydrazone compound was previously synthesized by Çakmak et al. to study its anticancer activity. Although non-original, this molecule was selected for evaluation in terms of its structure-activity relationship.²³ Additionally, the compound was characterized experimentally using various spectroscopic techniques, including FTIR,

$^1\text{H-NMR}$, and $^{13}\text{C-NMR}$. Furthermore, Hirshfeld surface analysis was performed computationally using Crystal Explorer 21.5.²⁴ An examination of the $\pi\cdots\pi$ contacts between the phenyl rings was also performed to enhance our understanding of molecular packing.

2. EXPERIMENTAL

Firstly, synthesis of the title compound was conducted. Then, FTIR and NMR experimental spectra were obtained. The structural determination and refinement processes were conducted using computer software specifically designed to solve the molecular crystal structures from single-crystal data obtained by X-ray diffraction.

2.1. Materials, methods, and instruments.

All chemicals were purchased from Merck and Sigma-Aldrich. The chemical purities of all compounds were checked by thin layer chromatography (TLC), employing a 20×20 cm alumina plate and a mobile phase consisting of a 1:1 mixture of petroleum ethyl acetate and hexane. Melting points were determined using a Schmelzpunktbestimmer SMP II melting point apparatus. FTIR spectra were recorded on a Shimadzu FTIR-8400 spectrometer. The $^1\text{H-NMR}$ and $^{13}\text{C-NMR}$ spectra were acquired using Bruker AV400 and Bruker Avance III spectrometers (300 MHz or 400 MHz), with tetramethylsilane (TMS) as the internal reference. Deuterated dimethylsulfoxide was used as the solvent for NMR. CHNS/O elemental analysis was performed using a Perkin-Elmer 2400 analyzer.

2.2. Chemistry

Hydrazide and its hydrazide-hydrazone derivative were synthesized from the starting material etofenamate. The structures of the synthesized compounds were confirmed through FTIR, $^1\text{H-NMR}$, $^{13}\text{C-NMR}$, and elemental analysis.

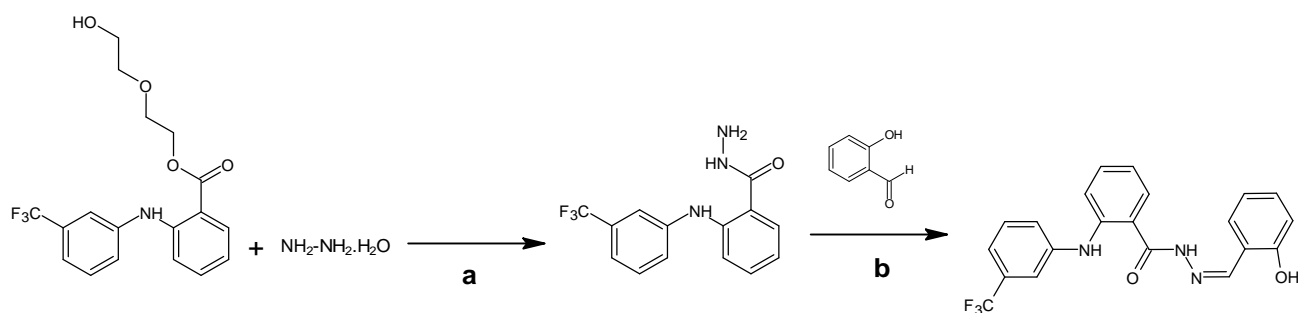


Fig. 1. General procedure for the synthesis of the compounds.

Reagent and conditions: (a) $\text{NH}_2\text{-NH}_2\cdot\text{H}_2\text{O}$, EtOH; (b) Substituted aldehydes, EtOH

2.3. Synthesis of hydrazone derivatives. Synthesis of 2-(3-(trifluoromethyl)anilino)benzohydrazide 1

The compound 2-((3-(trifluoromethyl)phenyl)amino)benzohydrazide 1 was prepared as previously described in the literature.^{25,26} Etofenamate (1 mmol) and an excess of hydrazine hydrate (99 %) (3 mmol) were mixed without solvent and heated at 110 – 120 °C for half an hour. To this mixture, EtOH (10 ml) was added, and the solution was heated in a water bath under reflux for 3 h. After cooling, the solid products formed were washed with water, filtered, recrystallized from ethanol, and dried.²⁷

(E)-N'-(2-hydroxybenzylidene)-2-((3-(trifluoromethyl)phenyl)amino)benzohydrazide

The compound 2-(3-(trifluoromethyl)anilino)benzohydrazide 1 synthesized in the first step was

used in the subsequent reaction. The hydrazide compound (1 mmol) was dissolved in 15 ml of ethanol. Then, 2-hydroxybenzaldehyde (1.2 mmol) was added, and the mixture was heated in a water bath for 4 hours. After heating, the solution was allowed to cool to RT. The resulting solid was recrystallized from ethanol.^{23,28}

(E)-N'-(2-hydroxybenzylidene)-2-((3-(trifluoromethyl)phenyl)amino)benzohydrazide

Yellow solid, yield 85%, mp 274 °C. FTIR ν_{max} (cm^{-1}): 3333 (O–H), 3173 (N–H), 3021 (aromatic C–H), 2877 (O–H \cdots N=C), 1622 (C=O), 1597 (C=N); $^1\text{H-NMR}$ (300 MHz, $\text{DMSO-}d_6$) δ 6.90 – 7.76 (m, 12H, Ar–H), 8.58 (s, 1H, –N=C–H), 9.22 (s, 1H, sec-amine), 11.27 (s, 1H, Ar–OH), 12.16 (s, 1H, O=C–NH); $^{13}\text{C-NMR}$ (100 MHz, $\text{DMSO-}d_6$) δ 114.20, 116.40, 117.06,

117.43, 118.59, 119.34, 120.20, 120.70, 121.57, 122.79, 125.49, 129.29, 129.47, 129.89, 130.21, 130.34, 131.43, 132.39, 142.56, 143.17, 148.29, 157.44, 164.33; Elemental analysis calculated for $C_{21}H_{16}F_3N_3O_2$: C, 63.16%; H, 4.04%; N, 10.52%. Measured C, 63.25%; H, 3.84%; N, 10.76%. The melting point of the compound was obtained using a Schmelzpunktbestimmer SMP II melting point apparatus. We obtained the material by crystallizing it in ethanol, determining its melting point as 274 °C. We believe that the difference between our findings and the melting point stated in the patent (74 °C) may be attributed to a typographical error or variations in the experimental conditions used. Different solvents can change the melting point by affecting molecular interactions and crystal structure. Crystallization of the material in different solvents can lead to significant differences in melting points. In addition, the purity of the material plays an important role; the melting point of a pure compound may differ from that of a compound containing impurities. Such discrepancies are especially likely given the differences in methods and conditions used.

2.4. FTIR, 1H -NMR, and ^{13}C -NMR spectra

In the FTIR spectrum of the hydrazone compounds, the C=O and C=N stretching bands were detected at 1622 cm^{-1} and 1597 cm^{-1} , respectively.^{23,29,30} The N–H stretching band of the hydrazone was observed at 3173 cm^{-1} (Fig. 1S).^{29,30} Additionally, the disappearance of the sharp bands characteristic of the hydrazide in the spectroscopic analysis confirmed the successful completion of the synthesis reaction. In the 1H -NMR spectrum, the absence of the peak expected for hydrazide and the increase in the number of aromatic protons indicate that the synthesis has occurred (Fig. 2S). In addition, the ^{13}C -NMR spectra of the hydrazone structures showed peaks at 164.33 ppm and 148.29 ppm,^{31,32} corresponding to the carbonyl and imine carbons, respectively (Fig. 3S).

2.5. Single-crystal structure determination and X-ray diffraction

A crystal of an appropriate size was selected and securely mounted on a suitable holder within a Bruker D8 Venture Photon II CMOS diffractometer.

Table 1

Crystal data and structure refinement for title compound

CCDC deposition number	2335288
Empirical formula	$C_{21}H_{16}F_3N_3O_2$
Formula mass ($\text{g} \cdot \text{mol}^{-1}$)	399.375
Radiation type, wavelength (Å)	Mo K_{α} radiation, $\lambda = 0.71073$
Temperature (K)	100
Crystal system	Monoclinic
Space group	P 2/n
Crystal color	Colourless
Unit cell dimensions (a, b, c) (Å)	21.0586(8), 8.1969(3), 21.6475(10)
Unit cell angles (α, β, γ)	$90^\circ, 92.886^\circ (2), 90^\circ$
Volume (Å^3)	3731.9(3)
Z	8
Density ρ (g/cm^{-3})	1.422
Absorption correction	Multi-scan
Absorption coefficient (μ)	0.114
Crystal size (mm^3)	$0.056 \times 0.069 \times 0.153$
F_{000}	1649.4
2θ range for data collection ($^\circ$)	$3.768 \leq \theta \leq 56.604$
Index ranges	$-28 \leq h \leq 25, -10 \leq k \leq 10, -28 \leq l \leq 28$
Reflections collected	96321
Independent/observed reflections	9257, 7890
$R_{\text{int}}, R_{\text{sigma}}$	0.0376, 0.0187
Goodness of fit on F^2	1.037
Final R indexes [$I \geq 2\sigma(I)$]	$R_1 = 0.0383, wR_2 = 0.0931$
Final R indexes [all data]	$R_1 = 0.0468, wR_2 = 0.0986$
Largest difference peak hole ($e/\text{Å}^{-3}$)	0.47/−0.35

The crystal structure of the molecule was determined using X-ray diffraction data. The structure was determined using Olex2-1.5 software³³ and with the SHELXT³⁴ structure solution program, which employs intrinsic phasing. Initially, the positions of the non-hydrogen atoms were refined anisotropically with SHELXL,³⁵ utilizing the full-matrix least-squares method for precise refinement. Subsequently, the positions of the hydrogen atoms were refined isotropically. A crystal information file (CIF) representing the molecule's structure was generated using WinGX.³⁶ Finally, the X-ray diffraction data in CIF format was deposited at the Cambridge Crystallographic Data Centre under accession number CCDC 2335288, ensuring accessibility for scientific reference and validation purposes. The details of the crystal data and the X-ray diffraction experiment are outlined in Table 1.

2.6. Computational methodology

Hirshfeld surface analysis is a powerful tool for visualizing and quantitatively evaluating intermolecular interactions in crystal structures. This method provides a three-dimensional representation of the molecular surface, enabling the examination of hydrogen bonds, Van der Waals interactions, and other weak interactions. For theoretical calculations, the crystal information file (CIF) for the molecule was generated using the WinGX-2014.1 program, and all computational processes were conducted using this file with the Crystal Explorer 21.5 software.

3. RESULTS AND DISCUSSION

3.1. XRD crystallography

The solid-state structure of the compound was verified through single-crystal X-ray diffraction (XRD) analysis. In the asymmetric unit of the compound, there are two crystallographically independent but chemically identical molecules, labeled as A and B, both of which are non-planar (Fig. 2a). The X-ray diffraction analysis of a single crystal indicates that the title compound possesses a monoclinic crystalline structure characterized by the P2/n space group. The unit cell dimensions are determined to be $a = 21.0586(8)$ Å, $b = 8.1969(3)$ Å, and $c = 21.6475(10)$ Å, with unit cell angles (α , β , γ) of 90° , $92.886(4)^\circ$, and 90° , respectively. The unit cell volume was calculated as $3731.9(3)$ Å³, and the number of molecules in the unit cell is $Z = 8$ (Fig. 2b). Molecular geometry calculations and drawings were performed using the Olex2-1.5 and Mercury software applications.³⁷

In the molecular structure of A and B, the following bond lengths were observed: C1-F2 (A: 1.3474 Å, B: 1.3430 Å); C6-N1 (A: 1.3947 Å, B: 1.4046 Å); N1-C8 (A: 1.3912 Å, B: 1.3825 Å); C9-C14 (A: 1.4908 Å, B: 1.4835 Å); C14-N2 (A: 1.3460 Å, B: 1.3486 Å); N2-N3 (A: 1.3835 Å, B: 1.3833 Å); and C15-C16 (A: 1.4495 Å, B: 1.4521 Å). All of these are single bonds. Other sources corroborate these findings, showing strong alignment with the calculated values of the compound: F2-C1 (1.336 Å),³⁸ N6-C20 (1.372 Å),³⁹ C8-N1 (1.383 Å),³⁸ C6-C7 (1.508 Å),⁴⁰ N2-C11 (1.357 Å),⁴¹ N2-N3 (1.339 Å),⁴² and C13-C17 (1.480 Å).⁴⁰

In addition, the double bond distances for C15=N3 and C14=O1 in the studied compound are as follows: C15=N3 (A: 1.2889 Å, B: 1.2890 Å) and C14=O1 (A: 1.2428 Å, B: 1.2452 Å), respectively. Similar results have been reported in the literature, indicating good agreement with the calculated values of the title compound: C10=N3 (1.282 Å)⁴³ and C1=O1 (1.231 Å).⁴² The XRD results of selected geometric parameters, along with these specified values, are presented in Table 2.

Table 2

Some selected geometric parameters from XRD results

Geometrical parameters	Molecule A	Molecule B
Bond length (Å)		
C1-C2	1.4970(19)	1.4950(20)
C1-F2	1.3474(16)	1.3430(18)
O1-C14	1.2428(14)	1.2452(14)
O2-C17	1.3536(17)	1.3528(15)
N1-C6	1.3947(16)	1.4046(15)
C14-N2	1.3460(15)	1.3486(15)
N3-N2	1.3835(13)	1.3833(14)
C15-N3	1.2889(16)	1.2890(16)
C3-C4	1.3880(20)	1.3830(20)
C21-C16	1.4041(18)	1.4016(18)
Bond angles (°)		
F2-C1-F1	105.79(11)	105.85(13)
C11-C12-C13	120.66(12)	121.10(12)
C6-N1-C8	128.47(11)	127.97(11)
O1-C14-N2	122.56(11)	122.31(11)
C14-N2-N3	119.67(10)	120.02(10)
C16-C17-O2	122.27(11)	122.09(11)
C19-C20-C21	118.82(13)	119.28(13)
Torsion angles (°)		
C15-C16-C17-C18	175.53(12)	177.40(12)
F1-C1-C2-C7	-123.36(14)	-97.55(12)
N1-C8-C12-C13	178.02(12)	174.07(12)
O1-C14-N2-N3	2.38(14)	2.64(14)

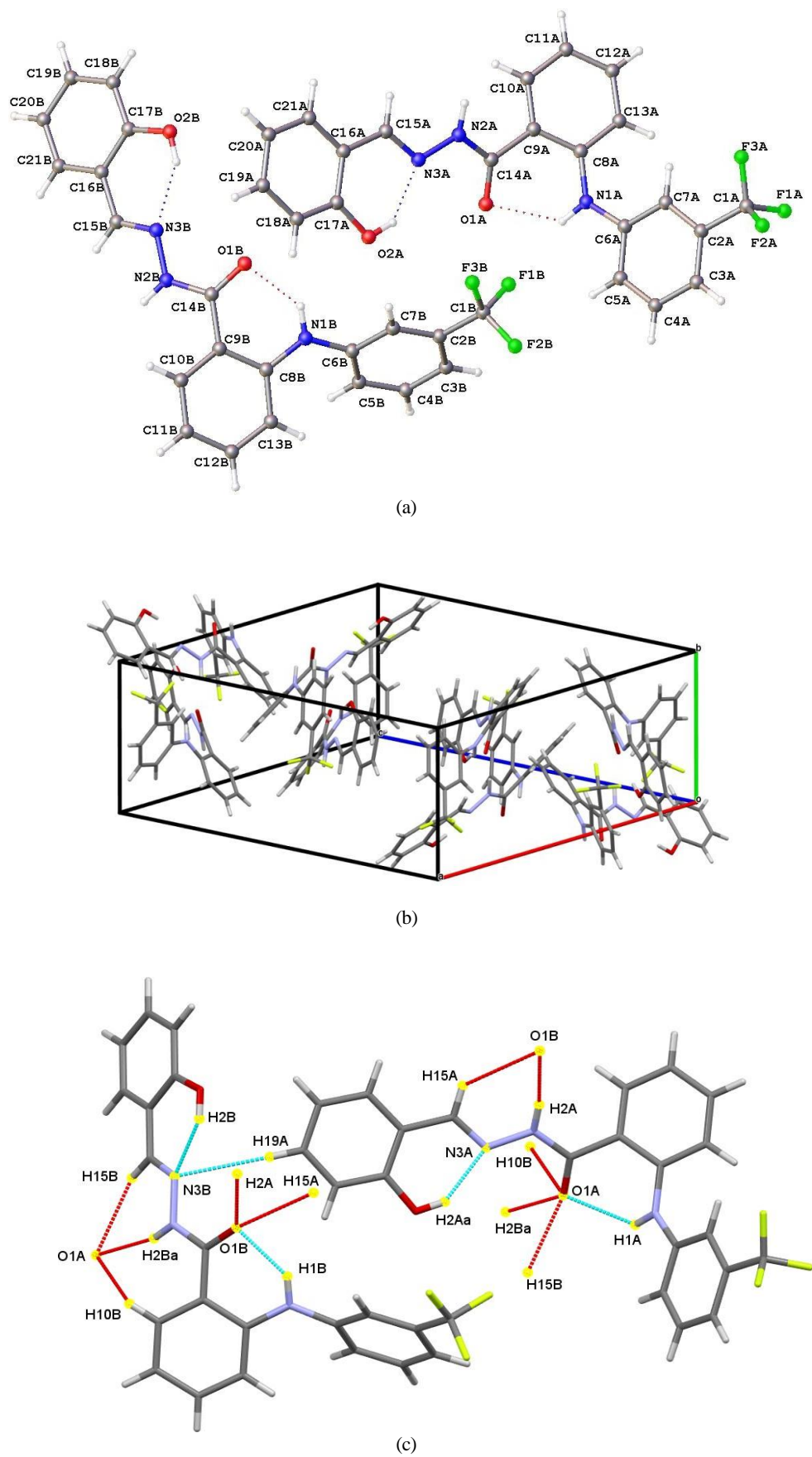


Fig. 2. (a) View of the title molecule, (b) crystal packing diagram, (c) crystal packing of the intermolecular hydrogen bonds of the studied compound

Furthermore, intramolecular H bonds were observed. The interaction bond lengths in molecular structures A and B are as follows: N3A-H2Aa (1.928 Å); O1A-H1A (2.177 Å); N3B-H2B (1.937 Å); and O1B-H1B (1.971 Å), as shown in Table 3.

The crystal structure reveals that the three phenyl rings (Ph1: C2/C7), (Ph2: C8/C13), and (Ph3: C16/C21) exhibit a planar conformation for both molecules A and B, with corresponding root mean square deviation (RMSD) values of 0.008, 0.004, and 0.009 for molecule A and 0.005, 0.018, and 0.003 for molecule B, respectively. X-ray diffraction measurements have shown that the dihedral angles between the rings are as follows: for molecule A, the angle between (Ph1 and Ph2), (Ph2 and Ph3), and (Ph1 and Ph3) are 41.88°, 21.25°, and 61.54°, respectively; for molecule B, the corresponding angles are 54.49°, 49.34°, and 68.31°, respectively.

3.2. Intermolecular geometric properties

The intermolecular geometric characteristics of the title compound involve a close-packed arrangement of its molecules. Table 3 displays selected bond length measurements for the compound. The examined molecule forms a six-membered ring due to intramolecular interactions between N3 and O1 atoms (N1A-H1A \cdots O1A^{#3}, N1B-H1B \cdots O1B^{#3}, O2A-H2Aa \cdots N3A^{#3}, and O2B-H2B \cdots N3B^{#3}), which enhance the stability of the crystal structure through strong hydrogen bonding. The crystal packing of the studied compound includes intermolecular hydrogen bonds, as illustrated in Figure 2c and Table 3: C15A-H15A \cdots O1B^{#1}; C15B-H15B \cdots O1A^{#2}; C10B-H10B \cdots O1A^{#2}; N2B-H2Ba \cdots O1A^{#2}; C19A-H19A \cdots N3B^{#3}; and N2A-H2Aa \cdots O1B^{#1}.

Table 3

Hydrogen-bond geometry

D-H \cdots A	(D-H)/Å	(H \cdots A)/Å	(D \cdots A)/Å	D-H \cdots A/deg.
C15A-H15A \cdots O1B ^{#1}	0.950	2.616	3.322	131.48
C15B-H15B \cdots O1A ^{#2}	1.289	2.425	3.217	126.52
C10B-H10B \cdots O1A ^{#2}	0.950	2.663	3.318	140.75
N2B-H2Ba \cdots O1A ^{#2}	0.872	1.980	2.824	162.36
C19A-H19A \cdots N3B ^{#3}	0.950	2.676	3.626	179.23
N2A-H2Aa \cdots O1B ^{#1}	0.908	2.676	2.778	170.49
N1A-H1A \cdots O1A ^{#3}	0.880	2.177	2.744	121.76
N1B-H1B \cdots O1B ^{#3}	0.880	1.971	2.682	136.84
O2A-H2Aa \cdots N3A ^{#3}	0.840	1.928	2.663	145.4
O2B-H2B \cdots N3B ^{#3}	0.840	1.937	2.674	145.95

Symmetry codes: ^{#1}-x+1, -y, -z+1; ^{#2}-x+1, -y+1, -z+1; ^{#3}x,y,z

$\pi\cdots\pi$ interactions play a crucial role in molecular packing, significantly influencing the arrangement of molecules. While intramolecular geometric characteristics provide insights into intermolecular hydrogen bonding, they may not explicitly address $\pi\cdots\pi$ interactions between phenyl rings of adjacent molecules. Using the Olex2 software for structural determination, calculations were performed to assess various parameters, including the distance between ring planes, the angle between ring planes, and the shift values between centers of the ring plane.

Our results reveal the presence of $\pi\cdots\pi$ interactions between the Ph3B-Ph1A, Ph1A-Ph1A and Ph3A-Ph3A phenyl rings within the molecule (Fig. 3). For the Ph3B-Ph1A ring planes, we obtained a centroid-centroid distance of 3.920 Å, a shift distance of 1.750 Å, and an angle between the ring planes of 3.925°. For the Ph1A-Ph1A ring planes, the centroid-centroid distance was 3.750 Å, the shift distance was 1.058 Å, and the angle between the ring planes was zero. Similarly, for the Ph3A-Ph3A ring planes, the centroid-centroid distance was 3.638 Å, the shift distance was 1.567 Å, and the angle between the ring planes was also zero.

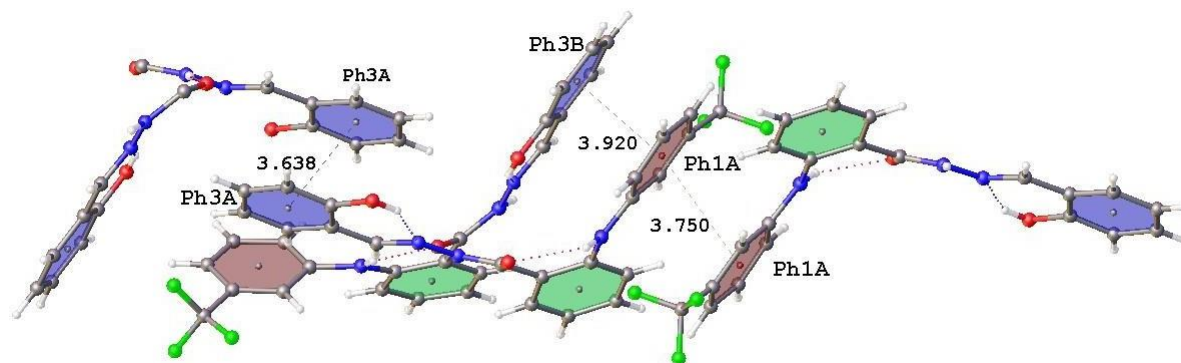


Fig. 3. $\pi\cdots\pi$ interactions between phenyl rings of neighboring molecules

3.3. Hirshfeld surface analysis

Hirshfeld surface analysis is a powerful method for investigating intermolecular atomic interactions within crystal structures.^{44–49} The three-dimensional (3D) Hirshfeld surface analysis is utilized to scrutinize these intermolecular interactions in the crystal environment through calculations and graphical representation. It is constructed by mapping the distance from each surface point to the nearest atom within the molecule.⁵⁰ The surface is then colored to reflect the attributes of the interatomic contacts.

The two-dimensional (2D) fingerprint map is a plot that shows the angle between two vectors (d_i and d_e), representing the directions of intera-

tomeric contacts in two dimensions when determining the d_{norm} . The d_{norm} represents the distance of a point on the Hirshfeld surface to the nearest atomic center, normalized by the sum of the van der Waals radii of the two atoms involved in the contacts. In this context, d_e denotes the distance from the closest atom outside the Hirshfeld surface, while d_i denotes the distance from the nearest atom inside this surface, respectively.⁵¹

Hirshfeld surface analysis was performed using Crystal Explorer 21.5 software. Figures 4 and 5 illustrate the Hirshfeld surfaces and 2D fingerprint maps for the two separate molecules (A and B). The d_{norm} plots were color-mapped, with values ranging from 1.2362 au (red) to 1.7394 au (blue).

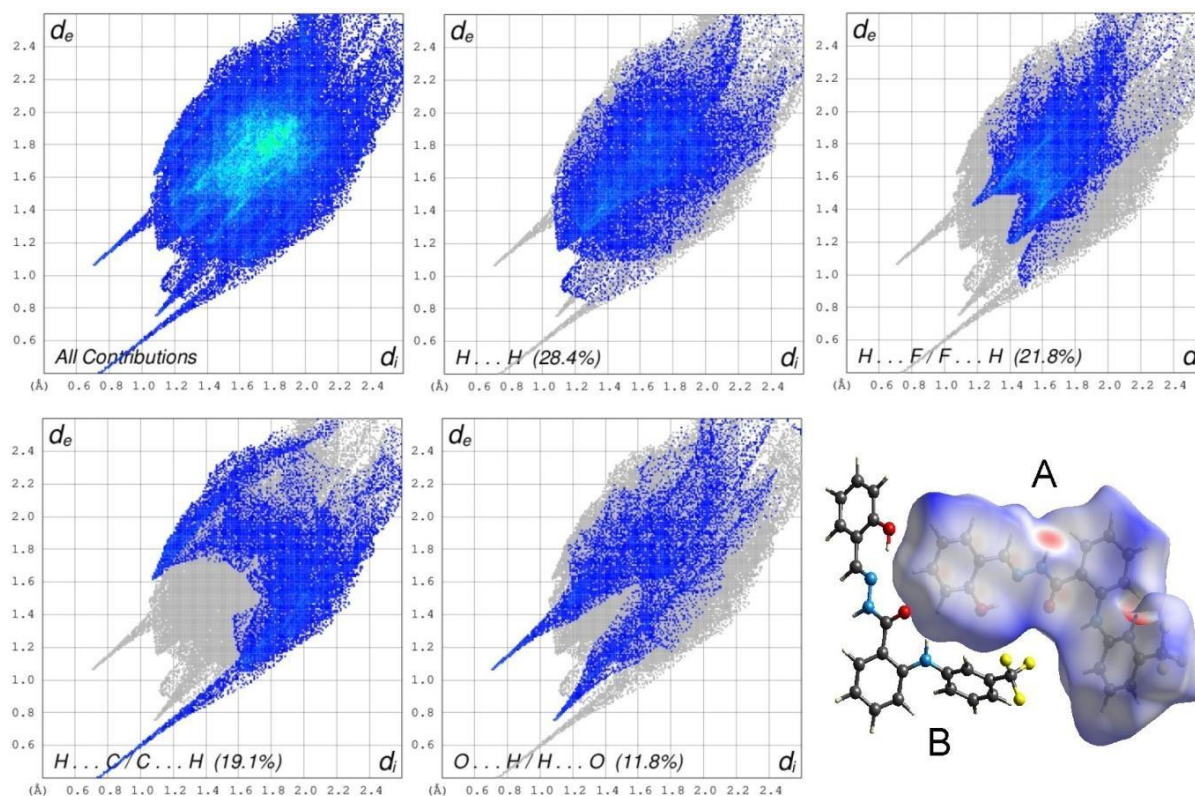


Fig. 4. Hirshfeld surface with d_{norm} and 2D fingerprint plots of molecule A

As seen in Figures 4 and 5, the investigation of intermolecular contacts on the Hirshfeld surface mapped at the d_{norm} value specific to the titled molecule revealed several prominent short dominant contacts, including C15A–H15A...O1B, C15B–H15B...O1A, C10B–H10B...O1A, N2B–H2Ba...O1A, C19A–H19A...N3B, and N2A–H2Aa...O1B. These interactions are represented in the dark red regions on the surface of the atoms, indicating areas where the distance between the atoms is smaller than the Van der Waals radii. Conversely, the blue regions highlight longer contact

points, while the white regions highlight contact points around the sum of the Van der Waals radii.⁵²

The 2D fingerprint maps provide a method to identify and summarize the various types of intermolecular contacts within the molecules. The 2D fingerprint plots indicate the presence of H...H (28.4 %), H...F/F...H (21.8 %), C...H/H...C (19.1 %), and O...H/H...O (11.8 %) close contacts in molecule A (Fig. 4). In contrast, molecule B displays H...H (31.5 %), C...H/H...C (23.6 %), H...F/F...H (23.3 %), and O...H/H...O (8.0 %) close contacts (Fig. 5).

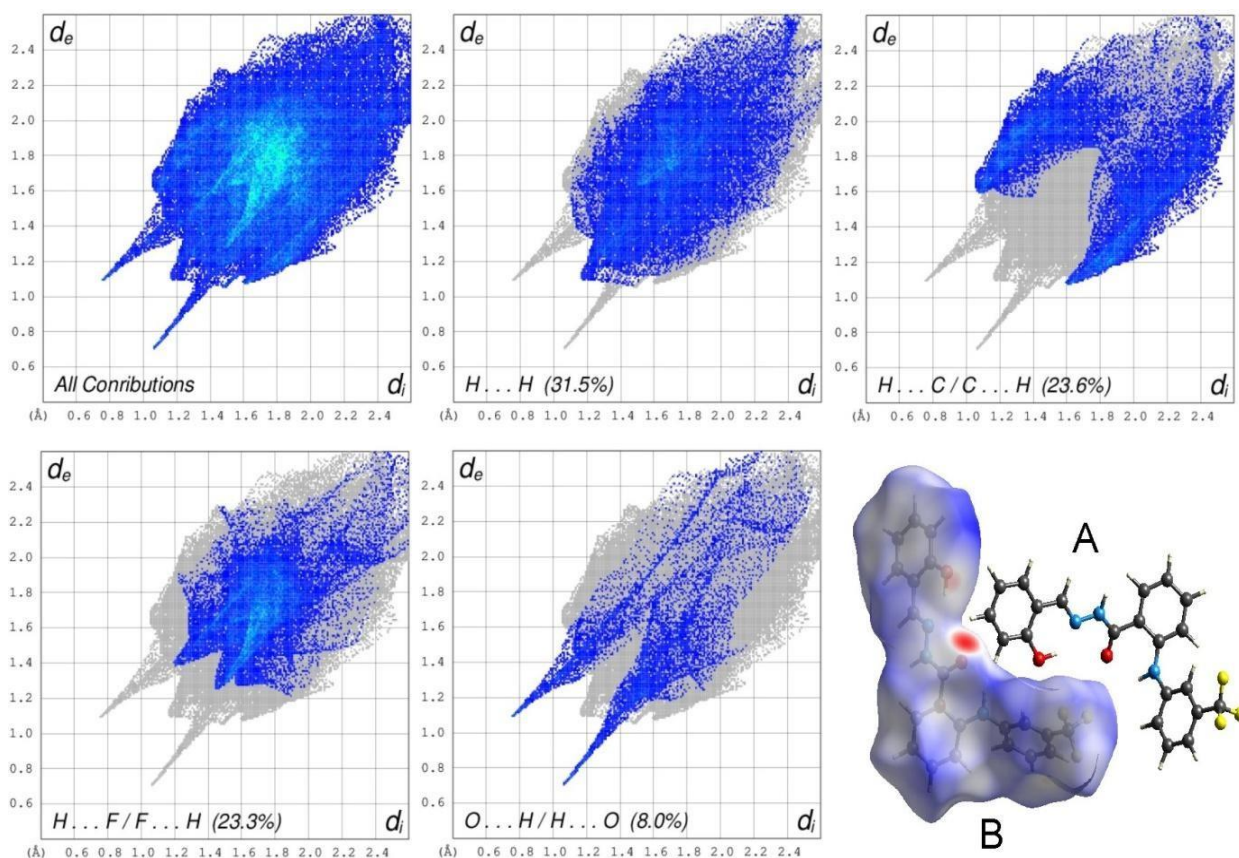


Fig. 5. Hirshfeld surface with d_{norm} and 2D fingerprint plots of molecule B

The total Hirshfeld surface area of the title compound highlights that H...H, C...H, F...H, and O...H contacts account for 81.1 % of the surface area for molecule A and 86.4 % for molecule B. These results offer valuable insights into the intermolecular contacts and arrangement within the crystal structures of the compound.

The shape index, along with red triangular concave regions and blue triangular convex regions, conveys information about each transmitter-

receiver pair.^{53,54} The intermolecular π ... π interactions occurring on the phenyl rings manifest as pairs of blue and red triangles organized in an "hourglass" configuration. The narrow sections and light-colored regions on the curvedness surface indicate weaker and longer contacts, in addition to hydrogen bonds.⁵⁵ In contrast, the π ... π interactions between molecular planes are represented as extensive flat regions of consistent green color (Fig. 6).

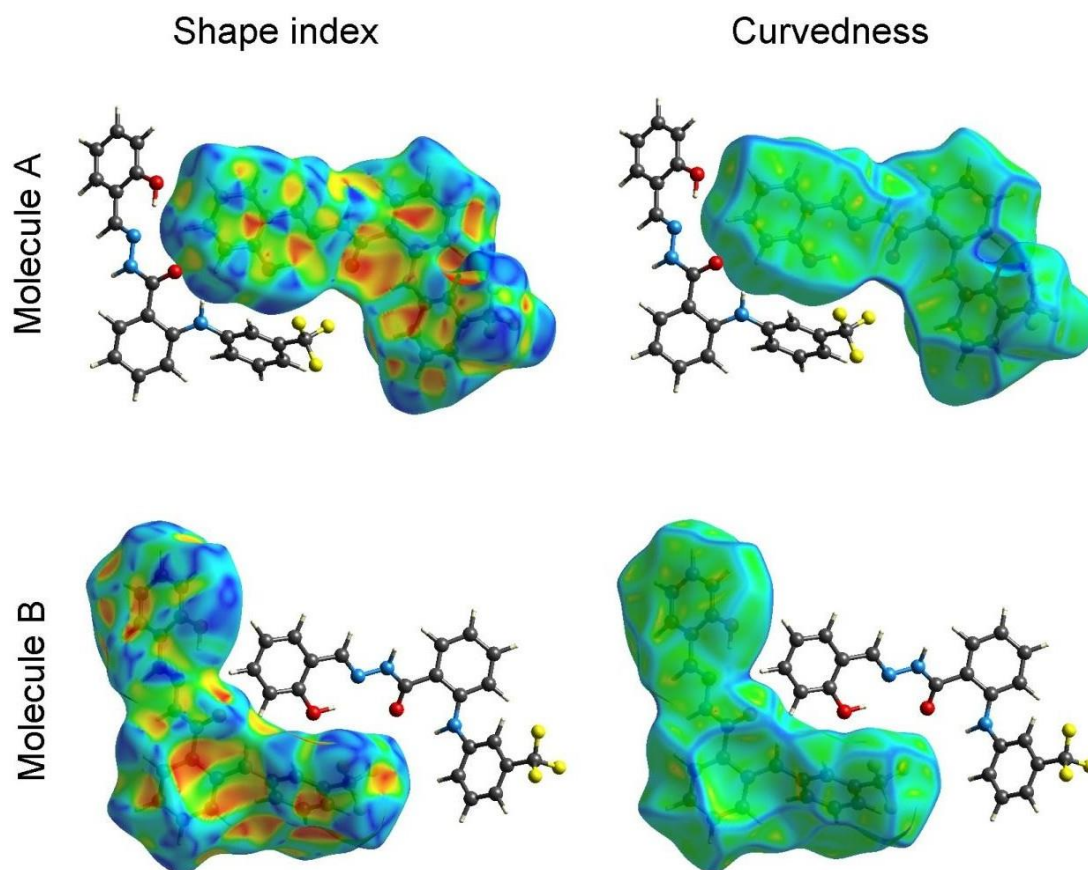


Fig. 6. Hirshfeld surfaces of molecules A and B with shape index and curvedness maps

4. CONCLUSIONS

(*E*)-*N'*-(2-hydroxybenzylidene)-2-((3-(trifluoromethyl)phenyl)amino)benzohydrazide was synthesized from the starting material etofenamate. The study investigated the structural properties of a hydrazide-hydrazone derivative, employing techniques such as XRD and spectroscopic methods including FTIR, $^1\text{H-NMR}$, and $^{13}\text{C-NMR}$. We determined that the compound consists of two crystallographically independent but chemically identical and non-planar molecules labeled A and B in its asymmetric unit, and that the title compound possesses a monoclinic crystal structure characterized by the P2/n space group.

Hirshfeld surface analysis was performed on the compound, revealing that predominant $\text{H}\cdots\text{H}$ contacts significantly influenced its crystal packing. Fingerprint plots were employed to discern the various types of intermolecular contacts existing on the Hirshfeld surface, showing that $\text{H}\cdots\text{H}$, $\text{C}\cdots\text{H}$, $\text{F}\cdots\text{H}$, and $\text{O}\cdots\text{H}$ contacts account for 81.1 % of the surface area for molecule A and 86.4 % for molecule B. While the stability of the crystal structure is enhanced by strong hydrogen bonds, $\pi\cdots\pi$ interactions also play an important role in packing.

The results indicate the existence of $\pi\cdots\pi$ interactions among the phenyl rings Ph3B–Ph1A, Ph1A–Ph1A, and Ph3A–Ph3A within the molecule, which can be readily observed from the shape index and curvedness diagrams. In summary, these findings provide valuable insights into the intermolecular interactions and crystal packing of (*E*)-*N'*-(2-hydroxybenzylidene)-2-((3-(trifluoromethyl)phenyl)amino)benzohydrazide, offering potential utility in understanding its properties and behaviors across diverse applications.

Conflicts of interest: The authors of this work declare that they have no conflicts of interest.

REFERENCES

- (1) Schiff, H., Mitteilungen aus dem Universitätslaboratorium in Pisa: eine neue Reihe organischer Basen. *Justus Liebigs Annalen der Chemie* **1864**, 131 (1), 118–119.
- (2) Tidwell, T. T., Schiff Hugo (Ugo), Schiff bases, and a century of β -lactam synthesis. *Angewandte Chemie International Edition* **2008**, 47 (6), 1016–1020.
- (3) Cimerman, Z.; Miljanić, S.; Galić, N., Schiff bases derived from aminopyridines as spectrofluorimetric analytical reagents. *Croatica Chemica Acta* **2000**, 73 (1), 81–95. <https://hrcak.srce.hr/132084>

- (4) Dhar, D. N.; Taploo, C., Schiff bases and their applications. *J Sci Ind Res.* **1982**, *41* (8), 501–506.
- (5) Rollas, S.; Güniz Küçükgül, Ş., Biological activities of hydrazone derivatives. *Molecules* **2007**, *12* (8), 1910–1939. <https://doi.org/10.3390/12081910>
- (6) Verma, G.; Marella, A.; Shaquiquzzaman, M.; Akhtar, M.; Ali, M. R.; Alam, M. M., A review exploring biological activities of hydrazones. *Journal of Pharmacy and Bioallied Sciences.* **2014**, *6* (2), 69–80. <https://doi.org/10.4103/0975-7406.129170>
- (7) Alhakimi, A. N., Synthesis, Characterization and microbicidal activities of *N*-(hydroxy-4-((4-nitrophenyl)diazenyl)benzylidene)-2-(phenylamino) acetohydrazone metal complexes. *Egyptian Journal of Chemistry* **2020**, *63* (4), 1509–1525. <https://doi.org/10.21608/ejchem.2020.20906.2256>
- (8) Uppal, G.; Bala, S.; Kamboj, S.; Saini, M., Therapeutic review exploring antimicrobial potential of hydrazones as promising lead. *Der Pharma Chemica* **2011**, *3* (1), 250–268.
- (9) Senthilkumar, S.; Seralathan, J.; Muthukumar, G., Synthesis, structure analysis, biological activity and molecular docking studies of some hydrazones derived from 4-aminobenzohydrazone. *Journal of Molecular Structure.* <https://doi.org/10.1016/j.molstruc.2020.129354>
- (10) Campbell, M. J., Transition metal complexes of thiosemicarbazide and thiosemicarbazones. *Coordination Chemistry Reviews* **1975**, *15* (2–3), 279–319. [https://doi.org/10.1016/S0010-8545\(00\)80276-3](https://doi.org/10.1016/S0010-8545(00)80276-3)
- (11) El-Sherif, A. A.; Shoukry, M. M.; Abd-Elgawad, M. M., Synthesis, characterization, biological activity and equilibrium studies of metal (II) ion complexes with tridentate hydrazone ligand derived from hydralazine. *Spectrochimica Acta, Part A: Molecular and Biomolecular Spectroscopy.* **2012**, *98*, 307–321. <https://doi.org/10.1016/j.saa.2012.08.034>
- (12) Suvarapu, L. N.; Seo, Y. K.; Baek, S.-O.; Ammireddy, V. R., Review on analytical and biological applications of hydrazones and their metal complexes. *E-Journal of Chemistry.* **2012**, *9* (3), 1288–1304. <https://doi.org/10.1155/2012/534617>
- (13) Merlani, M.; Nadaraia, N.; Amiranashvili, L.; Petrou, A.; Geronikaki, A.; Ciric, A.; Glamoclija, J.; Carevic, T.; Sokovic, M., Antimicrobial activity of some steroidal hydrazones. *Molecules* **2023**, *28* (3), 1167. <https://doi.org/10.3390/molecules28031167>
- (14) Sridhar, S. K.; Pandeya, S. N.; Stables, J. P.; Ramesh, A., Anticonvulsant activity of hydrazones, Schiff and Mannich bases of isatin derivatives. *European Journal of Pharmaceutical Sciences* **2002**, *16* (3), 129–132. [https://doi.org/10.1016/S0928-0987\(02\)00077-5](https://doi.org/10.1016/S0928-0987(02)00077-5)
- (15) Asif, M.; Husain, A., Analgesic, anti-inflammatory, and antiplatelet profile of hydrazones containing synthetic molecules. *J. Appl. Chem.* **2013**. <http://dx.doi.org/10.1155/2013/247203>
- (16) Chelucci, R. C.; Dutra, L. A.; Pires, M. E. L.; De Melo, T. R. F.; Bosquesi, P. L.; Chung, M. C.; Dos Santos, J. L., Antiplatelet and antithrombotic activities of non-steroidal anti-inflammatory drugs containing an N-acyl hydrazone subunit. *Molecules* **2014**, *19* (2), 2089–2099. <https://doi.org/10.3390/molecules19022089>
- (17) Bedia, K.-K.; Elçin, O.; Seda, U.; Fatma, K.; Nathaly, S.; Sevim, R.; Dimoglo, A., Synthesis and characterization of novel hydrazone-hydrazones and the study of their structure – antituberculosis activity. *European Journal of Medicinal Chemistry* **2006**, *41* (11), 1253–1261. <https://doi.org/10.1016/j.ejmech.2006.06.009>
- (18) Kumar, P.; Narasimhan, B., Hydrazides/hydrazones as antimicrobial and anticancer agents in the new millennium. *Mini Reviews in Medicinal Chemistry* **2013**, *13* (7), 971–987.
- (19) Su, X.; Aprahamian, I., Hydrazone-based switches, metallo-assemblies and sensors. *Chemical Society Reviews* **2014**, *43* (6), 1963–1981. <https://doi.org/10.1039/C3CS60385G>
- (20) Belowich, M. E.; Stoddart, J. F., Dynamic imine chemistry. *Chemical Society Reviews.* **2012**, *41* (6), 2003–2024. <https://doi.org/10.1039/C2CS15305J>
- (21) Spackman, M. A.; Jayatilaka, D., Hirshfeld surface analysis. *CrystEngComm.* **2009**, *11* (1), 19–32. <https://doi.org/10.1039/B818330A>
- (22) FERLUI Company, *New derivatives of O-amino substituted benzoylhydrazones*, French Republic National Industrial Property Institute (INPI) Paris, France. French Patent FR2168346A1, 1973.
- (23) Saral Çakmak, S.; Erdoğan, Ö.; Başoğlu, F.; Çoruh, U.; Çevik, Ö.; Karakuş, S., Exploring etofenamate hydrazone-hydrazone/copper(II) complexes: Synthesis, anticancer activity, carbonic anhydrase IX inhibition and docking studies. *Journal of Molecular Structure* **2024**, *1312*, 138555. <https://doi.org/10.1016/j.molstruc.2024.138555>
- (24) Spackman, P. R.; Turner, M. J.; McKinnon, J. J.; Wolff, S. K.; Grimwood, D. J.; Jayatilaka, D.; Spackman, M. A., CrystalExplorer: A program for Hirshfeld surface analysis, visualization and quantitative analysis of molecular crystals. *Journal of Applied Crystallography* **2021**, *54* (3), 1006–1011. <https://doi.org/10.1107/S1600576721002910>
- (25) Mali, S. N.; Thorat, B. R.; Gupta, D. R.; Pandey, A., Mini-review of the importance of hydrazides and their derivatives — synthesis and biological activity. *Engineering Proceedings* **2021**, *11* (1), 21. <https://doi.org/10.1016/j.bmc.2006.07.015>
- (26) Onnis, V.; Cocco, M. T.; Fadda, R.; Congiu, C., Synthesis and evaluation of anticancer activity of 2-arylamino-6-trifluoromethyl-3-(hydrazonocarbonyl)pyridines. *Bioorg Med Chem.* **2009**, *17* (17), 6158–65. <https://doi.org/10.1016/j.bmc.2009.07.066>
- (27) Nagender, P.; Kumar, R. N.; Reddy, G. M.; Swaroop, D. K.; Poornachandra, Y.; Kumar, C. G.; Narsaiah, B., Synthesis of novel hydrazone and azole functionalized pyrazolo[3,4-b]pyridine derivatives as promising anticancer agents. *Bioorganic & Medicinal Chemistry Letters.* **2016**, *26* (18), 4427–4432. <https://doi.org/10.1016/j.bmcl.2016.08.006>
- (28) Küçükgül, S. G.; Mazi, A.; Sahin, F.; Öztürk, S.; Stables, J., Synthesis and biological activities of diflunisal hydrazone-hydrazones. *European Journal of Medicinal Chemistry* **2003**, *38* (11–12), 1005–1013. <https://doi.org/10.1016/j.ejmech.2003.08.004>
- (29) Setyawati, A.; Wahyuningsih, T. D.; Purwono, B., Synthesis and characterization of novel benzohydrazone as

- potential antibacterial agents from natural product vanillin and wintergreen oil. *AIP Conference Proceedings* **2017**, 1823 (1). <https://doi.org/10.1063/1.4978194>
- (30) Suhta, A.; Saral, S.; Çoruh, U.; Karakuş, S.; Vazquez-Lopez, E. M., Synthesis, single crystal X-ray, Hirshfeld surface analysis and DFT calculation based NBO, HOMO–LUMO, MEP, ECT and molecular docking analysis of N'-[(2,6-dichlorophenyl)methylidene]-2-[[3-(Trifluoromethyl)phenyl]amino]benzohydrazide. *Journal of Structural Chemistry* **2024**, 65 (1), 196–215. <https://doi.org/10.1134/S0022476624010189>
- (31) Karthikeyan, M. S.; Prasad, D. J.; Poojary, B.; Subrahmanya Bhat, K.; Holla, B. S.; Kumari, N. S., Synthesis and biological activity of Schiff and Mannich bases bearing 2,4-dichloro-5-fluorophenyl moiety. *Bioorganic & Medicinal Chemistry* **2006**, 14 (22), 7482–7489. <https://doi.org/10.1016/j.bmc.2006.07.015>
- (32) Rollas, S.; Küçükgül, S. G., Biological activities of hydrazone derivatives. *Molecules* **2007**, 12 (8), 1910–1939. <https://doi.org/doi:10.3390/12081910>
- (33) Dolomanov, O. V.; Bourhis, L. J.; Gildea, R. J.; Howard, J. A.; Puschmann, H., OLEX2: a complete structure solution, refinement and analysis program. *Journal of Applied Crystallography* **2009**, 42 (2), 339–341. <https://doi.org/10.1155/2012/534617>
- (34) Sheldrick, G. M., SHELXT—Integrated space-group and crystal-structure determination. *Acta Crystallographica Section A: Foundations and Advances* **2015**, 71 (1), 3–8. <https://doi.org/10.1107/S2053273314026370>
- (35) Sheldrick, G. M., Crystal structure refinement with SHELXL. *Acta Crystallographica, Section C: Structural Chemistry* **2015**, 71(1), 3–8. <https://doi.org/10.1107/S2053229614024218>
- (36) Farrugia, L. J., WinGX and ORTEP for Windows: an update. *Journal of Applied Crystallography* **2012**, 45 (4), 849–854. <https://doi.org/10.1107/S0021889812029111>
- (37) Macrae, C. F.; Sovago, I.; Cottrell, S. J.; Galek, P. T.; McCabe, P.; Pidcock, E.; Platings, M.; Shields, G. P.; Stevens, J. S.; Towler, M., Mercury 4.0: from visualization to analysis, design and prediction. *Journal of Applied Crystallography* **2020**, 53 (1), 226–235. <https://doi.org/10.1107/S1600576719014092>
- (38) Suhta, A.; Saral, S.; Çoruh, U.; Karakuş, S.; Vazquez-Lopez, E., Synthesis, single crystal X-ray, Hirshfeld surface analysis and DFT calculation based NBO, HOMO–LUMO, MEP, ECT and molecular docking analysis of N'-[(2,6-dichlorophenyl)methylidene]-2-[[3-(trifluoromethyl)phenyl]amino]benzohydrazide. *Journal of Structural Chemistry* **2024**, 65 (1), 196–215. <https://doi.org/10.1134/S0022476624010189>
- (39) Arshad, M. N.; Bibi, A.; Mahmood, T.; Asiri, A. M.; Ayub, K., Synthesis, crystal structures and spectroscopic properties of triazine-based hydrazone derivatives: a comparative experimental-theoretical study. *Molecules* **2015**, 20 (4), 5851–5874. <https://doi.org/10.3390/molecules20045851>
- (40) Murugavel, S.; Ravikumar, C.; Jaabil, G.; Alagusundaram, P., Synthesis, crystal structure analysis, spectral investigations (NMR, FT-IR, UV), DFT calculations, ADMET studies, molecular docking and anticancer activity of 2-(1-benzyl-5-methyl-1H-1,2,3-triazol-4-yl)-4-(2-chlorophenyl)-6-methoxypyridine – a novel potent human topoisomerase II α inhibitor. *Journal of Molecular Structure* **2019**, 76, 729–742. <https://doi.org/10.1016/j.molstruc.2018.09.010>
- (41) Yildirim Gümüştan, I., Synthesis, crystal structure, Hirshfeld surface analysis and DFT studies of (Z)-1-(2-(4-nitrophenyl)hydrazineylidene)Naphthalen-2(1H)-One. *Journal of Structural Chemistry* **2023**, 64 (8), 1435–1447. <https://doi.org/10.1134/S0022476623080085>
- (42) Kaynak, F. B.; Özbey, S.; Karalı, N., Three novel compounds of 5-trifluoromethoxy-1H-indole-2,3-dione-3-thiosemicarbazone: Synthesis, crystal structures and molecular interactions. *Journal of Molecular Structure* **2013**, 1049, 157–164. <https://doi.org/10.1016/j.molstruc.2013.06.039>
- (43) Kaynar, N. K.; Yavuz, M.; Tanak, H.; Şahin, S.; Büyükgüngör, O.; Açar, E., Crystal structure of 2-(E)-(5-bromo-2-hydroxybenzylidene)hydrazono)-1,2-diphenylethanone. *Crystallography Reports* **2018**, 63, 375–378. <https://doi.org/10.1134/S1063774518030136>
- (44) Albayati, M. R.; Kansız, S.; Lgaz, H.; Kaya, S.; Dege, N.; Ali, I. H.; Salghi, R.; Chung, I.-M., Synthesis, experimental and theoretical characterization of (E)-2-((2,3-dimethylphenyl) amino)-N'-(furan-2-ylmethylene) benzohydrazide. *Journal of Molecular Structure* **2020**, 1219, 128518. <https://doi.org/10.1016/j.molstruc.2020.128518>
- (45) Al-Karawi, A. J. M.; OmarAli, A.-A. B.; Dege, N.; Kansız, S., Formation of a new CuII – triazole ester complex from 1,2-cyclohexanedione-bis(p-bromobenzohydrazone) compound as a consequence of copper(II)-catalyzed click reaction. *Chemical Papers* **2021**, 75, 3901–3914. <https://doi.org/10.1007/s11696-021-01614-x>
- (46) İlmi, R.; Kansız, S.; Al-Rasbi, N. K.; Dege, N.; Raithby, P. R.; Khan, M. S., Towards white light emission from a hybrid thin film of a self-assembled ternary samarium(III) complex. *New Journal of Chemistry* **2020**, 44 (15), 5673–5683. <https://doi.org/10.1039/C9NJ06287D>
- (47) Kansız, S.; Tolan, A.; Azam, M.; Dege, N.; Alam, M.; Sert, Y.; Al-Resayes, S. I.; İçbudak, H., Acesulfame based Co(II) complex: Synthesis, structural investigations, solvatochromism, Hirshfeld surface analysis and molecular docking studies. *Polyhedron* **2022**, 218, 115762. <https://doi.org/10.1016/j.poly.2022.115762>
- (48) Simsek, O.; Dincer, M.; Dege, N.; Saif, E.; Yilmaz, I.; Cukurovali, A. Crystal structure and Hirshfeld surface analysis of (Z)-4-[[4-(3-methyl-3-phenylcyclobutyl)thiazol-2-yl]amino]-4-oxobut-2-enoic acid. *Acta Crystallographica, Section E: Crystallographic Communications* **2022**, 78 (2), 120–124. <https://doi.org/10.1107/S2056989022000032>
- (49) Yağcı, N. K.; Kansız, S.; Özcandan, E., Synthesis, crystal structure, DFT studies, Hirshfeld surface analysis and drug delivery performance of bis(2-chloro-4,6-diaminopyrimidine) copper(II)-dichloride. *Journal of Molecular Structure* **2021**, 1246, 131142. <https://doi.org/10.1016/j.molstruc.2021.131142>
- (50) Acar, E.; Kansız, S.; Dege, N., Synthesis, crystal structure and Hirshfeld surface analysis of (E)-2-(4-methylbenzylidene)-N-phenylhydrazine-1-carbothioamide. *Journal of Structural Chemistry* **2023**, 64 (6), 974–983. <https://doi.org/10.1134/S0022476623060021>
- (51) Abdel-Aal, S. K.; Ouasri, A., Crystal structure, Hirshfeld

- surfaces and vibrational studies of tetrachlorocobaltate hybrid perovskite salts $\text{NH}_3(\text{CH}_2)_n\text{NH}_3\text{CoCl}_4$ ($n = 4, 9$). *Journal of Molecular Structure* **2022**, 1251, 131997. <https://doi.org/10.1016/j.molstruc.2021.131997>
- (52) Kurbanova, M.; Ashfaq, M.; Tahir, M.; Maharramov, A.; Dege, N.; Ramazanzade, N.; Cinar, E. Synthesis, crystal structure, supramolecular assembly inspection by Hirshfeld surface analysis and computational exploration of 4-phenyl-6-(p-tolyl)pyrimidin-2(1H)-One (PPTP). *Journal of Structural Chemistry* **2023**, 64 (3), 437–449. <https://doi.org/10.1016/j.molstruc.2021.131997>
- (53) Channabasappa, V.; Kumara, K.; Neratur, L. K.; Kariyappa, A. K. Synthesis, crystal structure studies and Hirshfeld surface analysis of 6-chloro-7-hydroxy-4-methyl-2H-chromen-2-one. *Chemical Data Collections* **2018**, 15, 134–142. <https://doi.org/10.1016/j.cdc.2018.05.005>
- (54) Spackman, M. A.; McKinnon, J. J.; Jayatilaka, D., Electrostatic potentials mapped on Hirshfeld surfaces provide direct insight into intermolecular interactions in crystals. *CrystEngComm*. **2008**, 10 (4), 377–388. <https://doi.org/10.1039/B715227B>
- (55) Naveen, S.; Kumara, K.; Al-Maqtari, H. M.; Urs, M. D.; Jamalis, J.; Reddy, K. R.; Lingegowda, N.; Lokanath, N., Synthesis, characterization crystal and molecular structure studies of 5-(3-methylbenzoyl)-4-methyl-1, 3, 4,5-tetrahydro-2H-1,5-benzodiazepin-2-one: Hirshfeld surface analysis and DFT calculations. *Chemical Data Collections* **2019**, 24, 100292. <https://doi.org/10.1016/j.cdc.2016.11.006>